

Linear Chain Compounds of Molybdenum(II) Acetate Linked by Pyrazine, 4,4'-Bipyridine, and 1,4-Diazabicyclo[2.2.2]octane

Makoto Handa,* Masahiro Mikuriya,*[†] Takanori Kotera,[†] Kori Yamada,
Tadahiro Nakao, Hiroki Matsumoto, and Kuninobu Kasuga

Department of Chemistry, Faculty of Science, Shimane University, Matsue 690

[†]Department of Chemistry, School of Science, Kwansei Gakuin University, Nishinomiya 662

(Received March 31, 1995)

A series of linear-chain complexes of molybdenum(II) acetate linked by bidentate bridging ligands, $[\text{Mo}_2(\text{O}_2\text{CCH}_3)_4\text{L}]_n$ (L=pyrazine (pyz), 4,4'-bipyridine (4,4'-bpy), and 1,4-diazabicyclo[2.2.2]octane (dabco)), have been prepared, and their crystal structures determined by an X-ray diffraction method. It has been shown that the relatively weak coordinations of the bridging ligands at the axial positions of $\text{Mo}_2(\text{O}_2\text{CCH}_3)_4$ (Mo–N=2.619 (8)–2.658(6) Å) can effectively control the arrangement of the dimer units to give chain structures with good linearities. No significant interactions between the dimer units have been observed.

As shown for Krogman salt, one-dimensional polymer complexes containing direct metal–metal interactions, i.e., metal–metal bonds, have unique physical (conductive, optical, and magnetic) properties.^{1,2)} However, the variety of the species is not very extensive, and practically converge into d^8 metal systems because they are essentially built up by stacks of planar complexes. Hanack et al. proposed a useful approach for polymer formation: They prepared a new type of one-dimensional conductors by arranging alternately metal phthalocyanine units and linear bidentate ligands with π -electrons.³⁾ Later, Collman et al. prepared the same type of polymers using metal porphyrins; they called them “shish-kebab” polymers, and reported that the partial oxidation extremely increased their conductivities.⁴⁾ This approach is very effective for constructing the polymers by combining the bridging ligands and metal complexes. If this approach is applied to control the arrangement of complexes having metal–metal bonds, it is possible to obtain polymers with metal–metal bonds. Our final goal is to produce an interaction between the metal–metal bond units. As a starting material, $\text{Mo}_2(\text{O}_2\text{CR})_4$ is feasible, because it easily allows axial coordination and its metal–metal bond is one of the most characterized ones.^{5,6)} Furthermore, the coordination sites lie at the trans positions of the $\text{Mo}_2(\text{O}_2\text{CR})_4$ molecule, which facilitates a linear structure favorable for the interaction. To date, some examples having linear structures have been reported for Cr, Rh, and Ru systems by using a combination of $\text{M}_2(\text{O}_2\text{CR})_4$ and linear bidentate ligands.^{7–9)} As for the Mo system, zigzag chains of $\text{Mo}_2(\text{O}_2\text{CCH}_3)_4$

units linked by non-linear bidentate ligands, (1,2-bis(dimethylphosphino)ethane (dmpe), tetramethylethylenediamine (tmed), *N,N'*-dimethylethylenediamine (*N,N'*-dmed), and 1,3-diaminopropane (pda)) have been reported.¹⁰⁾ However, no linear-chain compound has been reported for the Mo system. In the present study we selected pyrazine (pyz), 4,4'-bipyridine (4,4'-bpy), and 1,4-diazabicyclo[2.2.2]octane (dabco) as the linear bidentate ligand, and prepared linear-chain complexes of molybdenum(II) acetate ($\text{Mo}_2(\text{O}_2\text{CCH}_3)_4$ (1)), $[\text{Mo}_2(\text{O}_2\text{CCH}_3)_4(\text{pyz})]_n$ (2), $[\text{Mo}_2(\text{O}_2\text{CCH}_3)_4(4,4'\text{-bpy})]_n \cdot n\text{THF}$ (3), and $[\text{Mo}_2(\text{O}_2\text{CCH}_3)_4(\text{dabco})]_n$ (4). A preliminary account of this study has been previously reported.¹¹⁾

Experimental

Preparations of Complexes. Molybdenum(II) acetate ($\text{Mo}_2(\text{O}_2\text{CCH}_3)_4$ (1)) was prepared by a method described in the literature.¹²⁾

$[\text{Mo}_2(\text{O}_2\text{CCH}_3)_4(\text{pyz})]_n$ (2). A solution of pyz (187 mg, 2.34 mmol) in 4 ml of THF was added to a solution of molybdenum(II) acetate (100 mg, 0.234 mmol) in 4 ml THF under Ar, and was stirred for 1 h at room temperature. The separated orange powder was collected by filtration, washed with THF, and dried in vacuo. The yield was 60 mg. Anal. Found: C, 28.52; H, 3.06; N, 5.69%. Calcd for $\text{C}_{12}\text{H}_{16}\text{Mo}_2\text{N}_2\text{O}_8$: C, 28.36; H, 3.17; N, 5.51%.

$[\text{Mo}_2(\text{O}_2\text{CCH}_3)_4(4,4'\text{-bpy})]_n \cdot n\text{THF}$ (3). This compound was obtained as an orange powder by mixing THF solutions of molybdenum(II) acetate (100 mg, 0.234 mmol) and 4,4'-bpy (109 mg, 0.702 mmol) using a method similar to that of 2. The yield was 100 mg. Anal. Found: C, 40.10; H, 4.32; N, 4.31%. Calcd for $\text{C}_{22}\text{H}_{28}\text{Mo}_2\text{N}_2\text{O}_9$: C, 40.26; H,

4.30, N, 4.27%.

$[Mo_2(O_2CCH_3)_4(dabco)]_n$ (**4**). This compound was obtained as a pale-yellow powder by mixing THF solutions of molybdenum(II) acetate (100 mg, 0.234 mmol) and dabco (79 mg, 0.704 mmol) using a method similar to that of **2**. The yield was 70 mg. Anal. Found: C, 31.41; H, 4.75; N, 5.38%. Calcd for $C_{14}H_{24}Mo_2N_2O_8$: C, 31.13; H, 4.48; N, 5.19%.

Measurements. Elemental analyses for carbon, hydrogen, and nitrogen were carried out using a Yanaco CHN CORDER MT-5. Infrared spectra were measured on a Hitachi 260-50 infrared spectrometer. Raman spectra were obtained on a JASCO R-800 spectrometer in the solid state with 514.5 nm excitation. The electronic spectra were measured with a Shimadzu UV-3100 spectrophotometer.

X-Ray Crystal Structure Analysis. Crystals of **2**, **3**, and **4** suitable for a single-crystal X-ray structure determination were grown from a THF solution by a slow-diffusion technique using an H-shaped tube. Diffraction data were collected on an Enraf-Nonius CAD4 diffractometer using graphite-monochromated Mo $K\alpha$ radiation at 25 ± 1 °C. Crystal data and details concerning the data collection are given in Table 1. The lattice constants were determined by a least-squares refinement based on 25 reflections with $20 \leq 2\theta \leq 30^\circ$. The intensity data were corrected for Lorentz-polarization effects, but not for absorption. The structures were solved by direct methods. Refinements were carried out by full-matrix least-squares methods. All of the non-hydrogen atoms, except for THF of **3** and carbon atoms of dabco of **4**, were refined with anisotropic thermal parameters. The THF and dabco molecules were included in the full-matrix refinement with a disordered model. Hydrogen atoms of **2** and **4** were fixed at their calculated positions. For **3**, hydrogen atoms were not included in the calculation. A weighting scheme, $w = 1/[\sigma^2(|F_o|) + (0.02|F_o|)^2 + 1.0]$, was employed. The final discrepancy factors, $R = \sum ||F_o| - |F_c|| / \sum |F_o|$ and

$R_w = [\sum w(|F_o| - |F_c|)^2 / \sum |F_o|^2]^{1/2}$, are listed in Table 1. All of the calculations were carried out on a Micro-VAXII computer using an Enraf-Nonius SDP program package.¹³⁾ The atomic coordinates and thermal parameters of non-hydrogen atoms are listed in Table 2, and the selected bond distances and angles in Table 3. The anisotropic thermal parameters of non-hydrogen atoms, the atomic coordinates and temperature factors of hydrogen atoms, and the $F_o - F_c$ tables were deposited as Document No. 68041 at the Office of the Editor of Bull. Chem. Soc. Jpn.

Results and Discussion

The elemental analyses showed that all of the complexes have a stoichiometry $Mo_2(O_2CCH_3)_4:L = 1:1$. In the IR spectra of powder samples (KBr pellet) of **2**, **3**, and **4**, the O—C—O vibrations appear as a set of distinctive two bands in a very similar energy region to those of **1**, respectively ($\nu_{asym}(OCO) = 1530$ cm^{-1} , $\nu_{sym}(OCO) = 1440$ cm^{-1} for **2**; $\nu_{asym}(OCO) = 1530$ cm^{-1} , $\nu_{sym}(OCO) = 1430$ cm^{-1} for **3**; $\nu_{asym}(OCO) = 1530$ cm^{-1} , $\nu_{sym}(OCO) = 1440$ cm^{-1} for **4**).^{10,14,15)} From these facts, it was expected that the dimer skeletons were preserved upon a reaction with the bidentate ligands (pyz, 4,4'-bpy, and dabco) to form objective linear-chain structures.

The crystal structure of **2** is shown in Fig. 1. The structure of **2** comprises an infinite chain of $Mo_2(O_2CCH_3)_4$ units bridged by the pyz ligand. The crystallographic inversion centers are located at the midpoint of the Mo—Mo bonds and centers of the pyz molecules. The nitrogen atoms of pyz are weakly coordinated to the dimer unit with a distance of 2.658(6) Å. The $Mo_2(O_2CCH_3)_4$ unit is almost unperturbed by the coordination; the Mo—Mo bond distance (2.093(1) Å) is

Table 1. Crystal Data and Data Collection Details

	2	3	4
Formula	$Mo_2O_8N_2C_{12}H_{16}$	$Mo_2O_9N_2C_{22}H_{28}$	$Mo_2O_8N_2C_{14}H_{24}$
F.W.	508.15	656.35	540.23
Crystal system	Triclinic	Triclinic	Triclinic
Space group	$P\bar{1}$	$P\bar{1}$	$P\bar{1}$
$a/\text{\AA}$	8.178(2)	12.351(6)	8.091(5)
$b/\text{\AA}$	8.261(2)	14.434(8)	8.885(5)
$c/\text{\AA}$	7.628(4)	8.472(5)	7.864(5)
$\alpha/^\circ$	95.14(3)	107.13(3)	95.91(4)
$\beta/^\circ$	100.31(3)	110.08(3)	103.05(3)
$\gamma/^\circ$	60.27(2)	66.56(5)	62.89(5)
$V/\text{\AA}^3$	440.3	1279.4	490.2
Z	1	2	1
$D_c/g\text{ cm}^{-3}$	1.92	1.70	1.83
$D_m/g\text{ cm}^{-3}$	1.94	1.71	1.85
Crystal size/mm	0.12×0.30×0.55	0.25×0.28×0.38	0.20×0.35×0.45
$\mu(Mo\ K\alpha)/\text{cm}^{-1}$	14.3	10.1	12.9
2θ range/ $^\circ$	2.0—48.0	2.0—48.0	2.0—50.0
No. of reflections measured	1501	4410	1859
No. of unique reflections with $I > 3\sigma(I)$	1315	3426	1603
R	0.033	0.052	0.050
R_w	0.044	0.064	0.063

Table 2. Fractional Positional Parameters and Thermal Parameters of Non-Hydrogen Atoms with Their Estimated Standard Deviations in Parentheses

Atom	<i>x</i>	<i>y</i>	<i>z</i>	<i>B</i> _{eq} /Å ² ^{a)}	Atom	<i>x</i>	<i>y</i>	<i>z</i>	<i>B</i> _{eq} /Å ² ^{a)}
[Mo₂(O₂CCH₃)₄(pyz)]_n (2)									
Mo	0.8901(1)	0.0000(1)	0.4055(1)	2.16(1)	C6A	-0.0870(8)	0.4075(6)	0.386(1)	3.6(2)
O1	1.0898(6)	-0.2107(6)	0.2548(6)	3.2(1)	C6B	0.4120(8)	0.9075(7)	0.433(1)	3.7(2)
O2	0.8795(6)	0.2101(6)	0.2553(6)	3.1(1)	C7A	-0.0013(7)	0.4490(6)	0.502(1)	3.1(2)
O3	0.6774(6)	0.2081(6)	0.5451(6)	3.4(1)	C7B	0.4989(7)	0.9495(6)	0.445(1)	3.0(2)
O4	0.8861(6)	-0.2085(6)	0.5446(6)	3.4(1)	C8A	0.0829(9)	0.3931(7)	-0.372(1)	4.7(3)
N	0.6288(8)	-0.0006(8)	0.1424(7)	4.0(2)	C8B	0.5821(8)	0.8923(7)	0.345(1)	4.4(3)
C1	1.2623(9)	-0.2721(9)	0.3142(9)	3.4(2)	C9A	0.0772(9)	0.2978(7)	-0.374(1)	4.9(3)
C2	1.410(1)	-0.429(1)	0.216(1)	6.1(3)	C9B	0.5783(9)	0.7984(7)	0.249(1)	4.7(3)
C3	0.9904(9)	0.2728(9)	0.3145(9)	3.3(2)	OT1	0.315(3)	0.300(2)	0.180(4)	13.5(9)*
C4	0.981(1)	0.429(1)	0.217(1)	5.9(2)	OT2	0.228(3)	0.345(3)	0.252(4)	16(1)*
C5	0.657(1)	0.001(1)	-0.024(1)	5.0(2)	CT1	0.353(4)	0.241(3)	0.264(6)	13(1)*
C6	0.4749(9)	-0.001(1)	0.167(1)	5.0(2)	CT2	0.263(3)	0.159(3)	0.170(5)	10(1)*
[Mo₂(O₂CCH₃)₄(4,4'-bpy)]_n·nTHF (3)									
MoA	0.0124(1)	0.0696(1)	0.5090(1)	2.42(1)	CT3	0.178(3)	0.203(2)	0.076(4)	8.3(8)*
MoB	0.5124(1)	0.5696(1)	0.0729(1)	2.43(2)	CT4	0.316(4)	0.179(3)	0.086(5)	11(1)*
O1A	-0.1653(5)	0.1214(4)	0.3411(7)	3.2(1)	CT5	0.281(4)	0.289(3)	0.335(5)	11(1)*
O1B	0.3359(5)	0.6214(4)	0.1169(7)	3.0(1)	CT6	0.182(3)	0.233(3)	0.230(4)	9.1(9)*
O2A	-0.1900(5)	-0.0259(4)	0.3249(7)	3.2(1)	CT7	0.162(4)	0.326(3)	0.119(5)	12(1)*
O2B	0.3103(5)	0.4750(4)	-0.0387(7)	3.1(1)	CT8	0.227(4)	0.274(3)	0.039(5)	11(1)*
O3A	0.0852(5)	0.0100(4)	0.2939(7)	3.1(1)	[Mo₂(O₂CCH₃)₄(dabco)]_n (4)				
O3B	0.5851(5)	0.5109(4)	0.3020(7)	3.2(1)	Mo	0.1090(1)	0.0000(1)	0.1016(1)	2.80(1)
O4A	0.0579(5)	-0.1363(4)	0.2736(7)	3.3(1)	O1	-0.0901(8)	0.1964(7)	0.2341(8)	3.9(2)
O4B	0.5586(5)	0.3640(4)	0.1492(7)	3.1(1)	O2	0.1255(7)	0.1949(6)	-0.0193(8)	3.9(1)
NA	-0.0006(6)	0.2550(5)	-0.4917(9)	3.6(2)	O3	0.3207(7)	-0.1952(7)	-0.0192(8)	3.9(1)
NB	0.4976(7)	0.7559(5)	0.2448(9)	3.6(2)	O4	0.1065(8)	-0.1964(7)	0.2344(8)	4.0(1)
C1A	-0.2262(7)	0.0617(6)	0.283(1)	3.3(2)	N	0.3715(8)	-0.0004(7)	0.3701(8)	3.0(1)
C1B	0.2731(7)	0.5607(6)	0.054(1)	2.8(2)	C1	0.006(1)	0.256(1)	-0.160(1)	3.7(2)
C2A	-0.3521(9)	0.0947(8)	0.155(1)	5.2(3)	C2	-0.003(2)	0.408(1)	-0.240(2)	5.8(3)
C2B	0.1501(9)	0.5949(8)	0.088(1)	4.9(3)	C3	-0.262(1)	0.256(1)	0.160(1)	3.7(2)
C3A	0.0891(8)	-0.0797(7)	0.219(1)	3.4(2)	C4	-0.403(2)	0.407(1)	0.239(2)	5.9(3)
C3B	0.5880(8)	0.4194(7)	0.291(1)	3.3(2)	C5	0.505(3)	-0.177(3)	0.423(3)	5.9(5)*
C4A	0.128(1)	-0.1233(9)	0.053(1)	5.3(3)	C6	0.280(4)	0.131(3)	0.494(4)	7.5(7)*
C4B	0.628(1)	0.3776(8)	0.455(1)	5.2(3)	C7	0.501(4)	0.055(3)	0.303(4)	7.9(7)*
C5A	-0.0841(8)	0.3112(6)	0.392(1)	3.8(2)	C8	0.324(4)	-0.032(3)	0.535(4)	7.1(6)*
C5B	0.4155(8)	0.8118(7)	0.336(1)	3.8(2)	C9	0.563(4)	-0.113(3)	0.327(4)	7.6(7)*
					C10	0.359(3)	0.172(3)	0.395(3)	6.2(5)*

a) Anisotropically refined atoms are given in the form of the isotropic equivalent displacement parameter defined as: $(4/3)[\alpha^2 B(1,1) + b^2 B(2,2) + c^2 B(3,3) + ab(\cos \gamma)B(1,2) + ac(\cos \beta)B(1,3) + bc(\cos \alpha)B(2,3)]$. Starred atoms were refined isotropically with occupancy factor of 0.5.

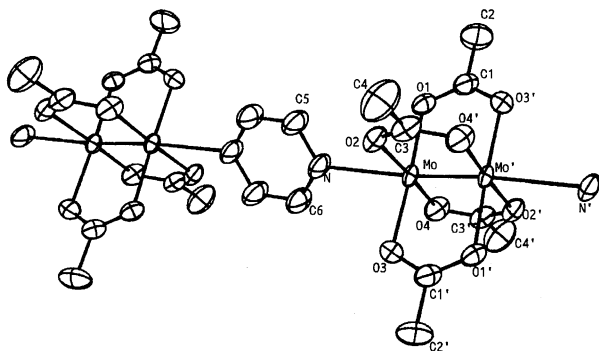


Fig. 1. Perspective view of the portion of the chain of [Mo₂(O₂CCH₃)₄(pyz)]_n (2). Primes refer to the equivalent positions (2-*x*, -*y*, 1-*z*).

similar to that in the parent complex **1** (2.0934(8) Å)¹⁶⁾ and the Mo-O bond lengths in **2** range from 2.118(4) to 2.124(4) Å, which are almost equivalent to those in **1** (2.107(5)–2.137(4) Å). The Mo'-Mo-N bond angle (174.7(2)°) shows the good linearity of the chain structure. The axial M-L bond length in **2** is 0.323 Å longer than that in [Cr₂(O₂CCH₃)₄(pyz)]_n.⁷⁾ This is not due to the difference in the radius of metal ion between the first and second transition metal, but is due to the different properties of Cr₂(O₂CR)₄ and Mo₂(O₂CR)₄ molecules to interact with the axial ligands; the tendency of Cr₂(O₂CR)₄ to bind the axial ligands is much stronger than that of Mo₂(O₂CR)₄.⁵⁾

In the case of **3**, the crystal consists of two crystallographically independent chains (designated as A and B hereafter). There is no remarkable structural

Table 3. Selected Bond distances (Å) and Angles (°) of **2**, **3**, and **4** with Their Estimated Standard Deviations in Parentheses

$[Mo_2(O_2CCH_3)_4(pyiz)]_n$ (2) ^{a)}			
Mo—Mo'	2.093(1)	Mo—O3	2.118(4)
Mo—O1	2.124(4)	Mo—O4	2.119(5)
Mo—O2	2.123(5)	Mo—N	2.658(6)
O1—Mo—O2	90.6(2)	O3—Mo—O4	89.7(2)
O1—Mo—O4	89.6(2)	O1—Mo—O3	176.4(2)
O2—Mo—O3	89.8(2)	O2—Mo—O4	176.5(2)
Mo'—Mo—N	174.7(2)		
$[Mo_2(O_2CCH_3)_4(4,4'$ -bpy)] _n · <i>n</i> THF (3) ^{b)}			
MoA—MoA'	2.103(1)	MoB—MoB''	2.104(1)
MoA—O1A	2.138(5)	MoB—O1B	2.132(6)
MoA—O2A	2.119(5)	MoB—O2B	2.120(6)
MoA—O3A	2.110(6)	MoB—O3B	2.109(6)
MoA—O4A	2.112(6)	MoB—O4B	2.117(6)
MoA—NA	2.619(8)	MoB—NB	2.624(7)
O1A—MoA—O3A	88.7(2)	O1B—MoB—O3B	88.3(2)
O1A—MoA—O4A	91.7(2)	O1B—MoB—O4B	91.9(2)
O2A—MoA—O3A	90.9(2)	O2B—MoB—O3B	91.2(2)
O2A—MoA—O4A	88.6(2)	O2B—MoB—O4B	88.5(2)
O1A—MoA—O2A	176.7(3)	O1B—MoB—O2B	176.9(2)
O3A—MoA—O4A	176.9(3)	O3B—MoB—O4B	176.8(2)
MoA'—MoA—NA	169.4(2)	MoB''—MoB—NB	169.0(2)
$[Mo_2(O_2CCH_3)_4(dabco)]_n$ (4) ^{c)}			
Mo—Mo'	2.095(1)	Mo—O3	2.129(5)
Mo—O1	2.132(5)	Mo—O4	2.134(7)
Mo—O2	2.128(7)	Mo—N	2.634(6)
O1—Mo—O2	86.7(3)	O3—Mo—O4	86.7(2)
O1—Mo—O4	93.5(3)	O1—Mo—O3	176.6(2)
O2—Mo—O3	92.9(3)	O2—Mo—O4	176.6(2)
Mo'—Mo—N	176.7(2)		

a) Primes refer to the equivalent positions (2−*x*, −*y*, 1−*z*). b) Primes and double primes refer to the equivalent positions (−*x*, −*y*, 1−*z*) and (1−*x*, 1−*y*, −*z*), respectively. c) Primes refer to the equivalent positions (−*x*, −*y*, −*z*).

difference between A and B. The A portion is depicted in Fig. 2. Crystallographic inversion centers are located at the midpoints of the Mo—Mo bonds and C—C bonds linking the two pyridyl rings of the bpy molecules. The weak axial coordinations of the nitro-

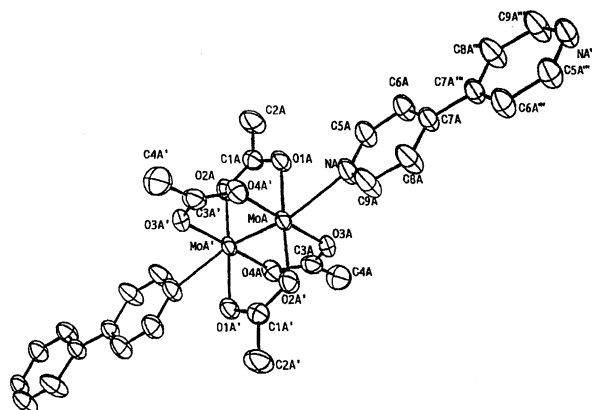


Fig. 2. Perspective view of the portion of the chain A of $[Mo_2(O_2CCH_3)_4(4,4'$ -bpy)]_n·*n*THF (**3**). Primes and triple primes refer to the equivalent positions (−*x*, −*y*, 1−*z*) and (−*x*, 1−*y*, 1−*z*), respectively.

gen atoms (MoA—NA=2.619(8) Å, MoB—NB=2.624(7) Å) do not affect the skeleton of the $Mo_2(O_2CCH_3)_4$ core; the Mo—Mo bond lengths are 2.103(1) (for A) and 2.104(1) Å (for B); Mo—O are 2.109(6)—2.138(5) Å. The Mo'—Mo—N bond angles are ∠MoA'—MoA—NA=169.4(2)°, ∠MoB'—MoB—NB=169.0(2)°. This fact indicates good linearities of the chain structures. A perspective view on the *bc* plane is shown in Fig. 3. Chain A is parallel to the *b*-axis, and chain B extends with an angle of 145.9° for the *b*-axis. THF molecules exist to fill the space in the crystal. This is in contrast with the case of the chain complex $[Mo_2(O_2C-t-Bu)_4(4,4'$ -bpy)]_n,¹⁷⁾ in which the *t*-butyl group may exclude any crystal solvent because of its bulkiness.

The crystal structure of **4** is shown in Fig. 4. The chains are elongated by alternating $Mo_2(O_2CCH_3)_4$ and dabco in a similar manner with **2**. The crystallographic inversion centers are located at the midpoints of the Mo—Mo bonds and centers of the dabco molecules. There are two orientations for the carbon atoms of dabco with two occupancies because of the existence of the inversion center in the center of dabco. In Fig. 4, only one of the two orientations are shown for clarity. The nitrogen atoms of dabco are coordinated to the dimer unit with a distance of 2.634(6) Å, almost com-

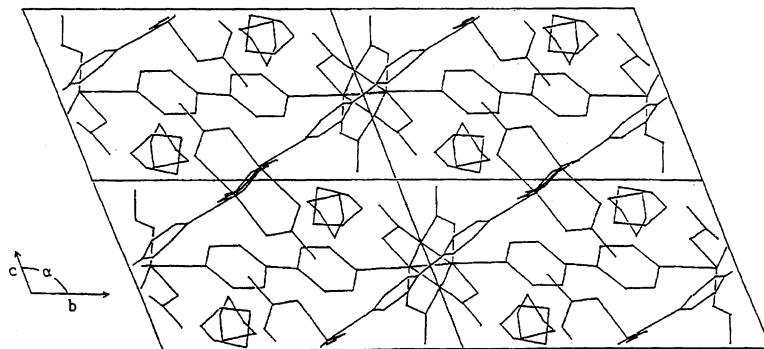


Fig. 3. Perspective view on *bc* plane of the chain structure of $[Mo_2(O_2CCH_3)_4(4,4'$ -bpy)]_n·*n*THF (**3**).

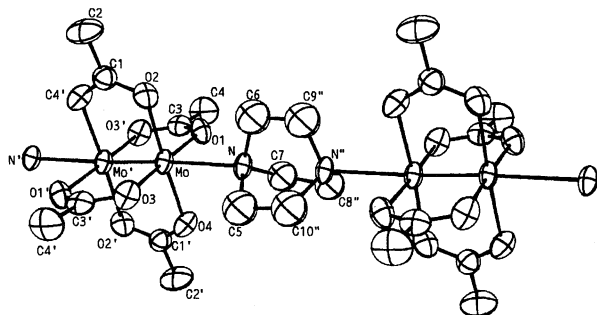


Fig. 4. Perspective view of the portion of the chain of $[\text{Mo}_2(\text{O}_2\text{CCH}_3)_4(\text{dabco})]_n$ (**4**). Primes and double primes refer to the equivalent positions $(-x, -y, -z)$ and $(1-x, -y, 1-z)$, respectively.

parable to those of **2** and **3**. That is, there is no considerable difference in the axial coordination strength between aromatic nitrogen and aliphatic nitrogen. This result suggests that the axial coordinations are essentially formed by σ -donations of the bridging ligands. The π -orbitals of the pyridine (of 4,4'-bpy) and pyrazine rings may not play an important role for the axial coordinations. The Mo–Mo bond distance is 2.905(1) Å and the Mo–O bond lengths are 2.127(7)–2.134(7) Å. Hence, the dimer skeleton of **4** is not affected by the axial coordination. The value of $\angle\text{Mo}'\text{--Mo--N}$, 176.7(2)° shows a good linearity of the chain structure.

In Table 4, some structural parameters of the chain complexes, $[\text{Mo}_2(\text{O}_2\text{CCH}_3)_4\text{L}]_n$ and the parent complex, $\text{Mo}_2(\text{O}_2\text{CCH}_3)_4$ (**1**), are summarized. The dimer skeletons of all the chain complexes are not affected by the axial coordinations. This is due to the strong Mo–Mo bond, which precludes any significant binding at the axial positions. In spite of the weak axial coordination, complexes **2**, **3**, and **4** show that the arrangement of the $\text{Mo}_2(\text{O}_2\text{CCH}_3)_4$ dimer units is efficiently controlled so as to produce a chain structure with good linearity. The geometrical linearity of the two nitrogen atoms of the bridging ligand is important to make a good linear chain structure.

In the solid-state Raman spectra, the Mo–Mo stretching bands of the present complexes are observed at 398 cm^{-1} for **2**, and 392 cm^{-1} for **3**

and **4**, respectively, slightly lower than that of **1** ($\nu_{\text{Mo--Mo}} = 403 \text{ cm}^{-1}$).¹⁸⁾ The shifts are small compared with those for pyridine (py) or 4,4'-bpy complexes of $\text{Mo}_2(\text{O}_2\text{CCF}_3)_4$; $\nu_{\text{Mo--Mo}} = 367 \text{ cm}^{-1}$ for $\text{Mo}_2(\text{O}_2\text{CCF}_3)_4(\text{py})_2$,¹⁹⁾ $\nu_{\text{Mo--Mo}} = 369 \text{ cm}^{-1}$ for $\{\text{Mo}_2(\text{O}_2\text{CCF}_3)_4\}_3(4,4'\text{-bpy})_4$,²⁰⁾ and $\nu_{\text{Mo--Mo}} = 394 \text{ cm}^{-1}$ for $\text{Mo}_2(\text{O}_2\text{CCF}_3)_4$. This is reflected in a lengthening of the Mo–Mo bond distances, accompanied by axial coordination; the Mo–Mo bonds for $\text{Mo}_2(\text{O}_2\text{CCF}_3)_4(\text{py})_2$ and $\{\text{Mo}_2(\text{O}_2\text{CCF}_3)_4\}_3(4,4'\text{-bpy})_4$ are stretched by 0.034–0.039 Å,^{19,20)} while those for **2**, **3**, and **4** by 0–0.02 Å. In $\text{Mo}_2(\text{O}_2\text{CCF}_3)_4(\text{py})_2$ and $\{\text{Mo}_2(\text{O}_2\text{CCF}_3)_4\}_3(4,4'\text{-bpy})_4$, electron-withdrawing fluorine atoms on the carboxylate may enhance the metal acidity, leading to relatively strong Mo–N bonds, giving a large elongation of Mo–Mo bonds, compared

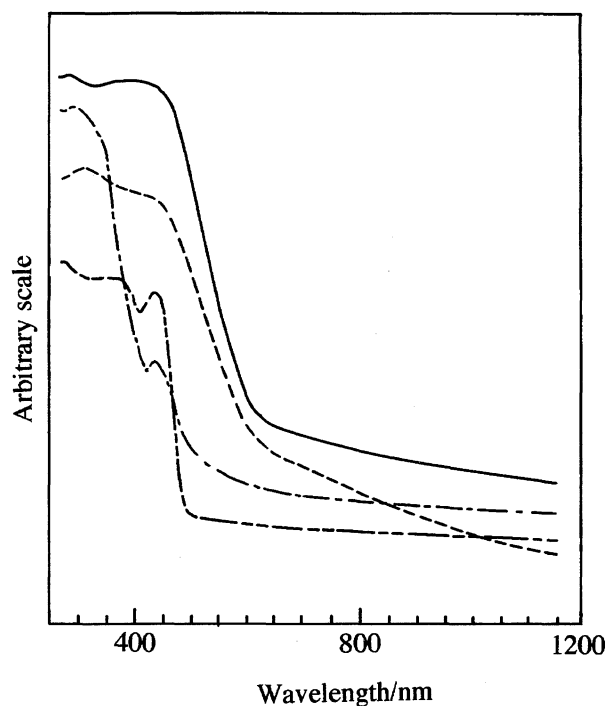


Fig. 5. Reflectance spectra of $[\text{Mo}_2(\text{O}_2\text{CCH}_3)_4(\text{pyz})]_n$ (**2**) (—), $[\text{Mo}_2(\text{O}_2\text{CCH}_3)_4(4,4'\text{-bpy})]_n \cdot n\text{THF}$ (**3**) (---), $[\text{Mo}_2(\text{O}_2\text{CCH}_3)_4(\text{dabco})]_n$ (**4**) (-.-), and $\text{Mo}_2(\text{O}_2\text{CCH}_3)_4$ (**1**) (....).

Table 4. Structural Parameters of $[\text{Mo}_2(\text{O}_2\text{CCH}_3)_4\text{L}]_n$ and the Parent Complex, $\text{Mo}_2(\text{O}_2\text{CCH}_3)_4$ (**1**)

Complex	Mo–Mo	Mo–O	Mo–N	Mo–Mo–N	Ref.
	Å	Å	Å	°	
$\text{Mo}_2(\text{O}_2\text{CCH}_3)_4$ (1)	2.0934(8)	2.119(5) ^{a)}			16
$[\text{Mo}_2(\text{O}_2\text{CCH}_3)_4(\text{pyz})]_n$ (2)	2.093(1)	2.121(5) ^{a)}	2.658(6)	174.7(2)	This work
$[\text{Mo}_2(\text{O}_2\text{CCH}_3)_4(4,4'\text{-bpy})]_n \cdot n\text{THF}$ (3)	2.104(1) ^{a)}	2.120(6) ^{a)}	2.622(8) ^{a)}	169.2(2) ^{a)}	This work
$[\text{Mo}_2(\text{O}_2\text{CCH}_3)_4(\text{dabco})]_n$ (4)	2.095(1)	2.131(7) ^{a)}	2.634(6)	176.7(2)	This work
$[\text{Mo}_2(\text{O}_2\text{CCH}_3)_4(\text{tmed})]_n$	2.103(1)	2.119(2) ^{a)}	2.729(2)	170.5(1)	10a
$[\text{Mo}_2(\text{O}_2\text{CCH}_3)_4(N,N'\text{-dmed})]_n$	2.102(1) ^{a)}	2.12(1) ^{a)}	2.69(1) ^{a)}	168.9(2) ^{a)}	10b
$[\text{Mo}_2(\text{O}_2\text{CCH}_3)_4(\text{pda})]_n$	2.103(1)	2.127(4)	2.636(11)	174.8(3)	10b

a) Mean values.

with **2**, **3**, and **4**.

Diffuse reflectance spectra of the present complexes show the band as a peak at 440 nm or a shoulder at around 450 nm (Fig. 5). This band has been assigned to a δ - δ^* transition based on the metal-metal bond.²¹⁾ These results are consistent with the facts that the $Mo_2(O_2CCH_3)_4$ dimer skeletons are retained in the polymer chains, as shown in the X-ray structure descriptions. However, there seems to be no remarkable interaction between the metal-metal bond units.

In order to produce an interaction through the bridging ligands, some trials for the chemical oxidation of the polymer complexes have been made. However, such efforts were in vain because of decompositions of the complexes which may occur due to the essential weakness of the ligations at the axial positions of $Mo_2(O_2CCH_3)_4$.

The present work was partially supported by a Grant-in-Aid for Scientific Research No. 06740508 from the Ministry of Education, Science and Culture.

References

- 1) K. Krogmann, *Angew. Chem., Int. Ed. Engl.*, **8**, 35 (1969).
- 2) "Extended Linear Chain Compounds," ed by J. S. Miller, Plenum, New York (1982), Vol. 1.
- 3) O. Schneider, J. Metz, and M. Hanack, *Mol. Cryst. Liq. Cryst.*, **81**, 273 (1982); M. Hanack, W. Kobel, J. Koch, J. Metz, O. Schneider, and H.-J. Schulze, *Mol. Cryst. Liq. Cryst.*, **96**, 263 (1983); O. Schneider and M. Hanack, *Angew. Chem., Int. Ed. Engl.*, **22**, 784 (1983); M. Hanack, *Mol. Cryst. Liq. Cryst.*, **105**, 133 (1984); B. N. Diel, T. Inabe, N. K. Jaggi, J. W. Lyding, O. Schneider, M. Hanack, C. R. Kannewurf, T. J. Marks, and L. H. Schwartz, *J. Am. Chem. Soc.*, **106**, 3207 (1984); M. Hanack, S. Deger, A. Lange, and T. Zippel, *Synth. Met.*, **15**, 207 (1986); U. Keppeler, S. Deger, A. Lange, and M. Hanack, *Angew. Chem., Int. Ed. Engl.*, **26**, 344 (1987); M. Hanack, S. Deger, U. Keppeler, A. Lange, A. Leverenz, and M. Rein, *Synth. Met.*, **19**, 739 (1987); M. Hanack, *Mol. Cryst. Liq. Cryst.*, **160**, 133 (1988).
- 4) J. P. Collman, J. T. McDevitt, G. T. Yee, C. R. Leidner, L. G. McCullough, W. A. Little, and J. B. Torrance, *Proc. Natl. Acad. Sci. U. S. A.*, **83**, 4581 (1986); J. P. Collman, J. T. McDevitt, G. T. Yee, M. B. Zisk, J. B. Torrance, and W. A. Little, *Synth. Met.*, **15**, 129 (1986); J. P. Collman, J. T. McDevitt, C. R. Leidner, G. T. Yee, J. B. Torrance, and W. A. Little, *J. Am. Chem. Soc.*, **109**, 4606 (1987).
- 5) F. A. Cotton and R. A. Walton, "Multiple Bonds between Metal Atoms," 2nd ed, Oxford Univ. Press, New York (1993).
- 6) J. L. Templeton, *Prog. Inorg. Chem.*, **26**, 211 (1979).
- 7) F. A. Cotton and T. R. Felthouse, *Inorg. Chem.*, **19**, 328 (1980).
- 8) F. A. Cotton and T. R. Felthouse, *Inorg. Chem.*, **20**, 600 (1981).
- 9) F. A. Cotton, Y. Kim, and T. Ren, *Inorg. Chem.*, **31**, 2723 (1992).
- 10) a) M. C. Kerby, B. W. Eichhorn, J. A. Creighton, and K. P. C. Vollhardt, *Inorg. Chem.*, **29**, 1319 (1990); b) B. W. Eichhorn, M. C. Kerby, K. J. Ahmed, and J. C. Huffman, *Polyhedron*, **10**, 2573 (1991).
- 11) M. Handa, K. Kasamatsu, K. Kasuga, M. Mikuriya, and T. Fujii, *Chem. Lett.*, **1990**, 1753.
- 12) T. A. Stephenson, E. Bannister, and G. Wilkinson, *J. Chem. Soc.*, **1964**, 2538.
- 13) B. A. Frenz, "The SDP-User's Guide," Enraf-Nonius, Delft, The Netherlands (1985).
- 14) W. K. Bratton, F. A. Cotton, M. Debeau, and R. A. Walton, *J. Coord. Chem.*, **1**, 121 (1971).
- 15) B. W. Eichhorn, M. C. Kerby, R. C. Haushalter, and K. P. C. Vollhardt, *Inorg. Chem.*, **29**, 723 (1990).
- 16) F. A. Cotton, Z. C. Mester, and T. R. Webb, *Acta Crystallogr., Sect. B*, **30**, 2768 (1974).
- 17) M. Handa, M. Mikuriya, R. Nukada, H. Matsumoto, and K. Kasuga, *Bull. Chem. Soc. Jpn.*, **67**, 3125 (1994).
- 18) J. S. Filippio, Jr., and H. J. Sniadoch, *Inorg. Chem.*, **12**, 2326 (1973); A. P. Ketteringham and C. Oldham, *J. Chem. Soc., Dalton Trans.*, **1973**, 1067.
- 19) F. A. Cotton and J. G. Norman, Jr., *J. Am. Chem. Soc.*, **94**, 5697 (1972).
- 20) M. Handa, K. Yamada, T. Nakao, K. Kasuga, M. Mikuriya, and T. Kotera, *Chem. Lett.*, **1993**, 1969.
- 21) W. C. Trogler and H. B. Gray, *Acc. Chem. Res.*, **11**, 232 (1978); D. S. Martin, R. A. Newman, and P. E. Fanwick, *Inorg. Chem.*, **18**, 2511 (1979); M. C. Manning, G. F. Holland, D. E. Ellis, and W. C. Trogler, *J. Phys. Chem.*, **87**, 3083 (1983).